J|A|C|S
ARTICLES
Published on Web 12/22/2005

Ab Initio Calculations of the Reaction Mechanisms for Metal−Nitride Deposition from Organo-Metallic Precursors onto Functionalized Self-Assembled Monolayers

Mohit Haran, James R. Engstrom, and Paulette Clancy*

Contribution from the School of Chemical and Biomolecular Engineering, Cornell University, Ithaca, New York 14853

Received July 13, 2005; E-mail: pqc1@cornell.edu

Abstract: An atomistic mechanism has been derived for the initial stages of the adsorption reaction for metal−nitride atomic layer deposition (ALD) from alkylamido organometallic precursors of Ti and Zr on alkyltrichorosilane-based self-assembled monolayers (SAMs). The effect of altering the terminal functional group on the SAM (including −OH, $-NH_2$, −SH, and $-NH(CH_3)$) has been investigated using the density functional theory and the MP2 perturbation theory. Reactions on amine-terminated SAMs proceed through the formation of a dative-bond complex with an activation barrier of 16−20 kcal/mol. In contrast, thiol-terminated SAMs form weak hydrogen-bonded intermediates with activation barriers between 7 and 10 kcal/mol. The deposition of Ti organometallic precursors on hydroxyl-terminated SAMs proceeds through the formation of stronger hydrogen-bonded complexes with barriers of 7 kcal/mol. Zr-based precursors form dative-bonded adducts with near barrierless transitions. This variety allows us to select a kinetically favorable substrate for a chosen precursor. The predicted order of reactivity of differently terminated SAMs and the temperature dependence of the initial reaction probability have been confirmed for Ti-based precursors by recent experimental results.[53] We predict that the replacement of methyl groups by trifluoromethyl groups on the SAM backbone decreases the activation barrier for amine-terminated SAMs by 5 kcal/mol. This opens a route to alter the native reactivities of a given SAM termination, in this case making amine termination energetically viable. The surface distribution of SAM molecules has a strong effect on the adsorption kinetics of Ti-based precursors. Unimolecular side decomposition reactions were found to be kinetically competitive with adsorption at 400 K.

1. Introduction

As the architecture of conventional electronic devices continues to shrink, the continued use of current inorganic materials will limit nanoscale device fabrication. One increasingly popular approach is to use the inherent tailorability offered by organic molecules in concert with current inorganic surfaces to develop molecular-scale devices. The use of self-assembled monolayers (SAMs) in both memory architectures and circuit elements is one such approach. SAMs offer the advantage of being able to control the functionality of the substrate by altering the terminal functional groups of SAMs, typically $-NH_2$, −OH, −SH, and −COOH. Ordered two-dimensional arrays of SAM end groups can be used as a template for uniform film growth for an interconnect formation between a metal contact and the underlying substrates in active devices such as molecular switches[1−3] and microelectronic interconnects.[4,5]

However, device applications composed of these unique organic interfaces will depend on having the ability to create ultrathin metallic interconnects for charge conduction to macroscopic metallic contacts or thin diffusion barriers acting as the gate dielectric for electrical transport in the plane of the substrate. Knowledge of the nature of the bonding of this inorganic/organic interface is essential to understand the details of charge transfer at these interfaces. Vapor deposition of metals on SAMs has been studied extensively, for example, Au, Ag, Cu, Al, and Ti deposition on alkanethiols and alkylsiloxane SAMs with a variety of organic functional end groups.[6−13] For the deposition of elemental species, penetration and degradation of the SAMs can occur with a highly reactive metal atom, such as Ti, necessitating a thin diffusion-barrier film.[1,14−17]

(1) Chen, J.; Reed, M. A.; Rawlett, A. M.; Tour, J. M. *Science* **1999**, *286*, 1550−1552.
(2) Yan, L.; Gao, Y. *Thin Solid Films* **2002**, *417*, 101−106.
(3) Ishii, H.; Sugiyama, K.; Ito, E.; Seki, K. *Adv. Mater.* **1999**, *11*, 605−625.
(4) Rossnagel, S. M. *J. Vac. Sci. Technol., B* **2002**, *20*, 2328−2336.
(5) Elam, J. W.; Wilson, C. A.; Schuisky, M.; Sechrist, Z. A.; George, S. M. *J. Vac. Sci. Technol., B* **2003**, *21*, 1099−1107.
(6) Jung, D. R.; Czanderna, A. W. *Crit. Rev. Solid State Mater. Sci.* **1994**, *19*, 1−54.
(7) Herdt, G. C.; Jung, D. R.; Czanderna, A. W. *Prog. Surf. Sci.* **1995**, *50*, 103−129.
(8) Tarlov, M. J. *Langmuir* **1992**, *8*, 80−89.
(9) Konstadinidis, K.; Zhang, P.; Opila, R. L.; Allara, D. L. *Surf. Sci.* **1995**, *338*, 300−312.
(10) Hooper, A. E.; Fisher, G. L.; Konstadinidis, K.; Jung, D.; Nguyen, H.; Opila, R. L.; Collins, R. W.; Winograd, N.; Allara, D. L. *J. Am. Chem. Soc.* **1999**, *121*, 8052−8064.
(11) Fisher, G. L.; Walker, A. V.; Hooper, A. E.; Tighe, T. B.; Bahnck, K. B.; Skriba, H. T.; Reinard, M. D.; Haynie, B. C.; Opila, R. L.; Winograd, N.; Allara, D. L. *J. Am. Chem. Soc.* **2002**, *124*, 5528−5541.
(12) Shin, H.; Collins, R. J.; De Guire, M. R.; Heuer, A. H.; Sukenik, C. N. *J. Mater. Res.* **1995**, *10*, 692−698.
(13) Shin, H.; Collins, R. J.; De Guire, M. R.; Heuer, A. H.; Sukenik, C. N. *J. Mater. Res.* **1995**, *10*, 699−703.

10.1021/ja054685k CCC: $33.50

Metal nitrides (TiN and TaN) represent promising candidates for interface applications. Depending upon the choice of the transition metal, and the stoichiometry of the layer that is formed, they can be either insulating (Ta_3N_5) or conducting (TaN)! They have also been used as effective diffusion-barrier materials and insulator caps on organic films, e.g., Zr_3N_4.[4,17−18] Highly conformal films of metal nitrides have been formed using chemical vapor deposition (CVD) of both halide-based precursors, such as $TiCl_4$[19−22] and $TaBr_5$,[23] and organometallic precursors, such as tetrakis-dimethylamido titanium {TDMAT or ($Ti(N(CH_3)_2)_4$)} and tetrakis-diethylamido titanium {TDEAT or ($Ti(N(C_2H_5)_2)_4$)}, with hydrogen plasmas and ammonia.[24−28] However, as device dimensions shrink and ultrathin conformal films are needed in high aspect ratio structures, such as vias, CVD lacks the control to deposit films at the low temperatures required for organic materials due to their poorer nucleation kinetics.[17] In contrast, atomic layer deposition (ALD)[29] is an ideal technique: metal oxides[30−32] and nitrides[19−23,25−27] deposited using halide precursors on inorganic substrates by ALD have been found to give excellent monolayer coverage, but the temperature requirements are too high (above 750 K) for applications involving organic layers such as SAMs, where thermal budgets are low.

Organometallic complexes of metals, such as alkylamido metal precursors (e.g., TDMAT), provide suitable alternative precursors for high deposition rates in ALD at low temperatures (<650 K).[30−33] In ALD, the initial chemisorbed monolayer forms the template for subsequent layers and determines properties such as packing density and step coverage.[15−17] Molecular-scale surface interactions between the organometallic precursor and the terminal functional groups that define the surface govern the kinetics of adsorption and provide an opportunity to tailor thermally activated chemistry for deposition on SAMs to create a desired reactivity. Despite the importance of molecular-scale interactions in ALD, we lack a detailed understanding of these interactions, hampering any attempt to optimize processing parameters and the ligand set to produce a desired deposited organometallic species. Of the few studies that have been conducted, there is no explicit examination of the reaction kinetics.[34−37] Ab initio quantum calculations offer an appropriate route to describe reaction mechanisms and qualitatively define the trends in deposition kinetics, for example, the reactivity trends for chemisorption of transition-metal complexes on organics.[33]

In this paper, we will probe reaction kinetics as we change the nature of the organometallic precursor and the chemistry of the self-assembled monolayers used as a substrate for the deposition of the metallic layer. We use ab initio computational methods to systematically investigate the initial reaction kinetics of the ALD of transition-metal nitrides of titanium and zirconium, formed from alkylamido-based organometallic precursors on organic substrates composed of SAMs with different terminal functional groups (−OH, −SH, or $-NH_2$). To our knowledge, this is first computational study which investigates (1) the influence of the nature of the SAM backbone, (2) the effect of the metal center of the organometallic precursor, and (3) the packing density of the SAM on the reaction pathway for organometallic deposition. These studies were investigated for a set of precursors including titanium (titanium tetramide ($Ti(NH_2)_4$), TDMAT, and TDEAT) and zirconium (zirconium tetramide ($Zr(NH_2)_4$) and tetrakis-dimethylamido zirconium**)**. Together, these studies provide an extensive description of the reaction landscape of the surface chemistry of ALD for early transition-metal nitrides on organic substrates. We expect this landscape to assist experimentalists in designing new precursors and conforming substrates for ultrathin film deposition of nitride films.

2. Methodology

Molecular orbital calculations were carried out using the Gaussian98 and Gaussian03 suite of programs.[38] Atomistic mechanisms, thermochemistry, and reaction kinetics were investigated using the B3LYP hybrid density functional theory (DFT) with Becke's exchange functional and the Lee−Yang−Parr correlation functional. DFT-based B3LYP methods have been found to be efficient and accurate for the study of molecular systems with the heavy atoms associated with organometallics. Because electronic structure calculations are computationally intensive, it is necessary to use small clusters to represent the chemically active portion of the substrate. We were able to represent the backbone of alkyl SAMs using small fragments, $CH_3CH_2CH_2$- and CH_3CH_2-, to lower our computational burden. Similarly, smaller molecular weight model precursors, titanium- and zirconium-tetramide, were generally used as computationally tractable representatives of larger precursors, such as TDMAT and TDMAZ. However, we did compute the reactivity of TDMAT and TDMAZ on SAMs to quantify the effect of precursor size. All of these studies considered the reactivity of the organometallic precursor with a single SAM molecule. However, to look at nonlocal effects on the reaction mechanism originating from the proximity of neighboring SAM molecules packed onto a surface, the SAM substrate was modeled as a cluster consisting of multiple SAM molecules attached to a small fragment of a Si (100)−(2 × 1)

(14) de Boer, B.; Frank, M. M.; Chabal, Y. J.; Jiang, W.; Garfunkel, E.; Bao, Z. *Langmuir* **2004**, *20*, 1539−1542.
(15) Fisher, G. L.; Hooper, A. E.; Opila, R. L.; Allara, D. L.; Winograd, N. *J. Phys. Chem. B* **2000**, *104*, 3267−3273.
(16) Hooper, A.; Fisher, G. L.; Konstadinidis, K.; Jung, D.; Nguyen, H.; Opila, R.; Collins, R. W.; Winograd, N.; Allara, D. L. *J. Am. Chem. Soc.* **1999**, *121*, 8052−8064.
(17) Kim, H. *J. Vac. Sci. Technol., B* **2003**, *21* (6), 2231−2261.
(18) Hoffman, D. M. *Polyhedron* **1994**, *13* (8), 1169−1179.
(19) Ritala, M.; Leskela, M.; Rauhala, E.; Haussala, P. *J. Electrochem. Soc.* **1995**, *142*, 2731−2737.
(20) Elers, K.; Saanila, E.; Soininen, P. J.; Li, W.-M.; Kostamo, J. T.; Haukka, S.; Juhanojo, J.; Besling, W. F. A. *Chem. Vap. Deposition* **2002**, *8*, 149−153.
(21) Kim, H.; Rossnagel, S. M. *J. Vac. Sci. Technol., A* **2002**, *20*, 802−808.
(22) Rossnagel, S. M.; Sherman, A.; Turner, F. *J. Vac. Sci. Technol., B* **2000**, *18*, 2016−2020.
(23) Chen, X.; Frisch, H. L.; Kaloyeros, A. E.; Arkles, B. *J. Vac. Sci. Technol., B* **1998**, *16*, 2887−2890.
(24) Sun, S. C.; Tsai, M. H. *Thin Solid Films* **1994**, *253*, 440−444.
(25) Yun, J.; Park, M.; Rhee, S. *J. Electochem. Soc.* **1999**, *146* (5), 1804−1808.
(26) Min, J.-W.; Son, Y.-W.; Kang, W.-G.; Chun, S.-S.; Kang, S.-W *Jpn. J. Appl. Phys., Part 1* **1998**, *37*, 4999−5004.
(27) Yun, J.-H.; Choi, E.-S.; Jang, C. M.; Lee, C.-S. *Jpn. J. Appl. Phys., Part 2* **2002**, *41* (4a), L418−L421.
(28) Kim, D.-J.; Jung, Y.-B.; Lee, M.-B.; Lee, Y.-H.; Lee, J.-H. *Thin Solid Films* **2000**, *372*, 276−283.
(29) Suntola, T.; Hyvarinen, J. *Annu. Rev. Mater. Sci.* **1985**, *15*, 177−195.
(30) Aarik, J.; Aidla, A.; Uustare, T.; Ritala, M.; Leskela, M. *Appl. Surf. Sci.* **2000**, *161*, 385−395.
(31) Kukli, K.; Ritala, M.; Sajavaara, T.; Keinonen, J.; Leskela, M. *Chem. Vap. Deposition* **2002**, *8* (5), 199−204.
(32) Seo, E. K.; Lee, J.-W.; Sung-Suh, H. M.; Sung, M. M. *Chem. Mater.* **2004**, *16*, 1878−1883.
(33) Xu, Y.; Musgrave, C. B. *Chem. Mater.* **2004**, *16*, 646−653.
(34) Nissen, T. P.; Bill, J.; Aldinger, F. *Chem. Mater.* **2001**, *13*, 1552−1559.
(35) Fischer, R. A.; Weckenmann, U.; Winter, C.; Kashammer, J.; Scheumann, V.; Mittler, S. *J. Phys. IV* **2001**, *11*, Pr3/1183−Pr3/1190.
(36) Weiss, J.; Himmel, H. J.; Fischer, R. A.; Woell, C. *Chem. Vap. Deposition* **1998**, *4*, 17−21.
(37) Wohlfart, P.; Weiss, J.; Kashammer, J.; Kreiter, M.; Winter, C.; Fischer, R.; Mittler-Neher, S. *Chem. Vap. Deposition* **1999**, *5*, 165−170
(38) Frisch, M. J. et al. Gaussian 03, Revision C.02; Gaussian, Inc.: Wallingford, CT, 2004.

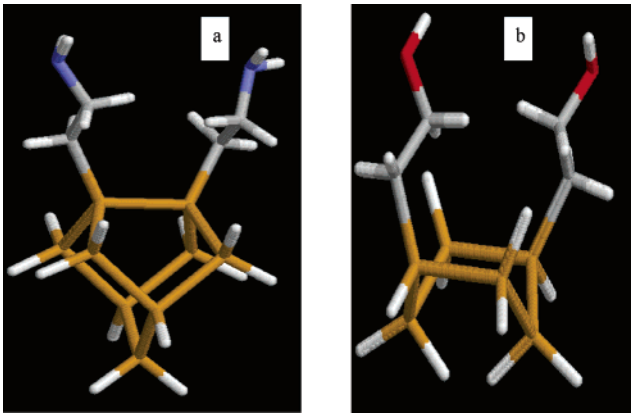

Figure 1. (a) Si_9H_{12} single-dimer cluster with two $-NH_2$ SAM molecules attached; (b) S_6H_{10} two-dimer cluster, referred to as a "diagonal dimer," with two −OH SAM molecules.

substrate that reproduced the local bonding arrangement of the bulk silicon substrate. We used two representative clusters, Si_9H_{12} (Figure 1a) and Si_6H_{10} (referred to subsequently as the "diagonal dimer" configuration, Figure 1b) to study the effect of packing density (25%, 50%, and 100%). These clusters are the largest "surface" we were able to study. In these studies, we have neglected interactions between coadsorbed species. Nonlocal electronic effects of Si (100) surfaces are effectively screened by the SAM covering the Si substrate, validating the use of smaller clusters as a template for the packing of SAMs. To obtain the model clusters, an initial bulk hydrogen-terminated Si (100)−(2×1) surface containing 208 atoms was relaxed in a system containing periodic boundary conditions using orthogonal tight binding[39] to account for bulk constraints. Model clusters were then obtained by truncating the optimized structures and terminating any Si−Si dangling bonds with hydrogen atoms to satisfy the sp^3 termination of Si atoms. These H-terminated clusters were then reoptimized using DFT methods with boundary conditions maintaining the angular orientations of terminating hydrogen atoms to mimic those in the Si bulk. This is similar in spirit to the procedure adopted successfully by Widjaja and Musgrave.[40]

The electronic structure was expanded over the 6-311G(d) and 6-311+G(d) basis sets for all the atoms during geometry optimization calculations of amide and dimethylamido-based precursors, respectively. In surface calculations, the basis set 6-311G(d) was used for all of the atoms in the Si (100)−dimer cluster. For the diagonal dimer, the chemically active portion of the SAMs and the precursor were expanded over the 6-311G(d) basis set, whereas the Si substrate was expanded on the 6-31G(d) basis set. The energetics calculated at this basis set were found to be within ±1 kcal/mol of values obtained for the larger basis set 6-311+G(d,p), verifying the accuracy of our choice. In the absence of an all-electron basis set for Zr, they were expanded using LANL2DZ effective core potentials (ECP), which consist of the Los Alamos LANL2 ECP and a valence double-ζ basis set. The electronic structure of other atoms in the Zr-based precursors were expanded over the 6-311G(d) and 6311G+(d) Gaussian basis sets. Structural data produced for TDMAZ from our calculations are in good agreement with experimental data from electron diffraction.[41,42] The reliability of the LANL2DZ pseudopotential was tested by comparing the potential energy diagram (PED) for reactions of titanium-based precursors expanded using full basis sets with those obtained by the expansion of the LANL2DZ pseudopotential over Ti. We found good agreement (within 1 kcal/mol) for the PED of the reaction. Frequency calculations on the optimized geometries of reaction intermediates, products, and

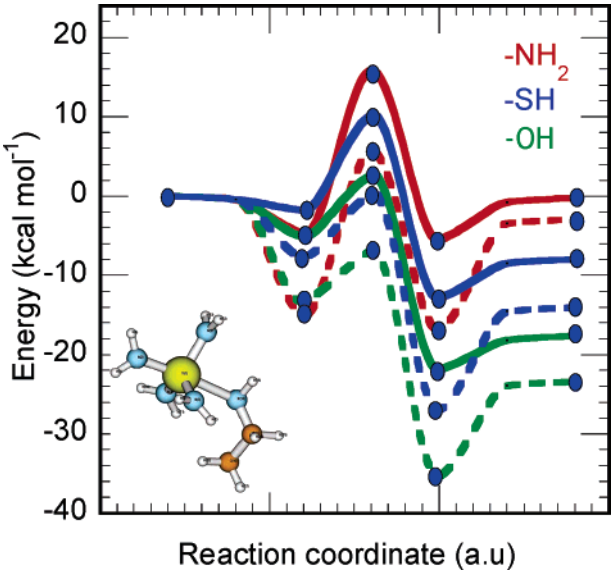

Figure 2. PED for reaction of titanium tetramide on $-NH_2$, −OH, and −SH SAMs at MP2/6-311G(d)//B3LYP/6-311G(d) (dashed lines) and B3LYP/6-311++G(d,p)//B3LYP/6-311G(d) (solid lines) model chemistries. (Inset) Distorted trigonal-bipyramidal structure of the adduct complex for amines.

reactants were scaled by a factor of 0.961 to calculate zero-point energies.[40] Normal-mode analysis was used to verify the stationary state and correct transition state. Vibrational frequencies obtained from these calculations were used to obtain partition functions which were applied with the conventional transition state theory (TST) to obtain reaction rates. Single point calculations using 6-311++G(d,p) and 6-311+G-(d,p) basis sets over the optimized structures were performed for the gas phase and surface reactions, respectively, to obtain more accurate energetic and activation barriers. The energy differences predicted in the present work have a mean absolute deviation of no more than 4 kcal/mol at the chosen model chemistries, compared to experimental data. These were corrected for basis set superposition error by including the counterpoise correction. DFT-based methods, such as B3LYP, have been observed to underestimate binding/adsorption energies.[43] Ab initio-based MP2 methods are effective but much more computationally costly. Single-point energy calculations using MP2/6-311G(d) were carried out to rectify any underestimation of adsorption energies.

3. Results and Discussion

3.1. TDMAT Deposition on Amine-Terminated SAMs. The PED for the reaction of titanium tetramide on amine-terminated SAMs in the gas phase is shown in Figure 2. The Ti-based precursor initially forms a dative-bond adduct on the amine termination between the amine group on the SAM and the Ti atom of the precursor. This is accompanied by a distortion of the precursor from tetrahedral to trigonal-bipyramidal geometry. Adduct formation is exothermic by 5 and 15 kcal/mol without the zero-point correction, using B3LYP/6-311++G(d,p) and MP2/6-311G(d), respectively. The transition state involves the transfer of a hydrogen atom from the amine group on the SAM to the amine ligand on the metal precursor through a four-center Ti−N−H−N in a distorted trigonal-bipyramidal geometry,[33,44] with an activation barrier of 18 kcal/mol (compared to 17 kcal/mol by a similar computational study[44]) with respect to the entry-channel adduct (the reactant adduct on the reaction pathway)

(39) Goringe, C. M.; Bowler, D. R.; Hernandez, E. *Rep. Prog. Phys.* **1997**, *60*, 1447−1512.
(40) Widjaja, Y.; Musgrave, C. B. *Surf. Sci.* **2000**, *469*, 9−20.
(41) Russo, T. V. *J. Phys. Chem.* **1995**, *99*, 17085−17087.
(42) Hagen, K.; Holwill, C. J.; Rice, D. A.; Runnacles, J. D. *Inorg. Chem.* **1988**, *27*, 2032−35.
(43) Siodmiak, M.; Frenkink, G.; Korkin, A. *J. Mol. Model.* **2000**, *6*, 413−424.
(44) Cross, J. B.; Schlegel, H. B. *Chem. Mater.* **2000**, *12*, 2466−2474.

for all of the model chemistries. The reaction byproduct, ammonia, is molecularly adsorbed to the product through a dative bond with a binding energy of 5 kcal/mol.[44]

To understand the effect of precursor size on chemical reactivity and choice of the basis set, we investigated the reaction energetics of three titanium precursors with increasingly bulky side-ligand groups (TDMAT and TDEAT) with methylamine. The same reaction mechanism was found to hold for all of the precursors. The adduct binding energy was found to decrease with an increase in side-ligand size (Table S1; Supporting Information) with both reactant and product side adducts equally destabilized. The decrease in binding energy can be attributed to an increased steric hindrance from bulkier side ligands on the precursor and higher electron donation to titanium from more electron-donating side ligands, reducing the strength of the dative bond with an amine group on the SAM. This is manifested in the elongation of the Ti−N dative bond length from 2.40 to 2.48 to 2.56 Å on replacing titanium tetramide with TDMAT and TDEAT, respectively. The activation barrier with respect to the entry-channel adduct was found to be unaffected by precursor size (Table S1). As a result, the reaction barriers for titanium tetramide, TDMAT, and TDEAT with respect to the vacuum were found to be 7, 10, and 17 kcal/mol, respectively, calculated using MP2/6-311G(d), which is in agreement with the experimentally observed activation barriers (8−10 kcal/mol for TDMAT and 15 kcal/mol for TDEAT).[23−24,45] These activation barriers suggest a reduction in deposition kinetics with an increase in precursor bulkiness at low precursor partial pressure (henceforth called "low pressure") deposition conditions, where the activation barrier would be defined with respect to the vacuum. The invariance of the activation barrier with respect to the adduct suggests the dominance of local chemical interactions between the metal and the terminal group of the SAM in determining the transition state and, thus, the activation barrier at high precursor pressure, under which conditions a fast equilibrium between the precursor and adduct can be assumed. On the basis of this observation, we are able to use titanium- and zirconium-tetramide as models for the study of activated reaction kinetics of larger organometallics under high-pressure deposition conditions.

The adsorption energy results using MP2/6-311+G(d)//B3LYP/6-311G(d) were found to be approximately equal to those obtained by using MP2/6-311+G(d)//B3LYP/6-311+G(d) and the computationally less expensive MP2/6-311G(d))//B3LYP/6-311G(d). The activation barriers with respect to the reactant side adduct, calculated using B3LYP/6-311G(d), B3LYP/6-311+G(d), B3LYP/6-311++G(d,p), and MP2/6-311G(d) on structures optimized on B3LYP/6-311G(d) and B3LYP/6-311+G(d), were found to be relatively insensitive to the model chemistry used (Table S1). To reduce computational costs, we chose B3LYP/6-311+G(d) as the model chemistry for optimization and frequency calculations of reaction pathways for smaller precursors, such as titanium tetramide, and used B3LYP/6-311G(d) for larger precursors. Increases in the chain length of the SAM were found to have a negligible effect on the adduct formation energy and activation barrier with respect to the entry-channel adduct beyond a single alkyl group. This suggests that using a chain containing even two alkyl groups can represent the SAM's reactive backbone. This was validated by comparison to the reaction profile of an eight-carbon backbone SAM with smaller chains. The effect of surface attachment of the SAM on the potential-energy surface of the reaction was investigated by depositing titanium tetramide on an ethylamine SAM attached to a Si (100) single-dimer cluster. The reaction mechanism and activation energy were found to be very similar (∼1 kcal/mol) to the PED for the corresponding gas-phase reaction, suggesting negligible surface effects at low packing densities of SAMs.

3.1.2. TDMAT Deposition on Hydroxyl- and Thiol-Terminated SAMs. Reaction mechanisms for the deposition of titanium tetramide and TDMAT on −OH- and −SH-terminated SAMs were found to be very similar, with the formation of hydrogen-bonded intermediates. (Note the contrast to the dative-bond intermediate observed for $-NH_2$-terminated SAMs.) Hydrogen bonding occurs between the amido group of the organometallic species and a hydroxyl group on the SAM with a binding energy of 5.5 kcal/mol using B3LYP/6-311++G(d,p) (Figure 2). As a result, the organometallic species retains tetrahedral geometry with an elongation of the amine bond involved in the hydrogen bond, from 1.90 to 1.95 Å. A dative-bonded intermediate formed by the organometallic species with a hydroxyl-terminated SAM, analogous to the $-NH_2$ adduct, was found to be thermodynamically unstable compared to the hydrogen-bonded intermediate in terms of ΔG (by ∼5 kcal/mol). The reaction has a low activation barrier of 7 kcal/mol relative to the hydrogen-bonded adduct, with the distorted trigonal-bipyramidal transition state lying near the vacuum level. In this geometry, the Ti−O bond distance is reduced sharply from 3.90 to 2.16 Å, with concomitant elongation in the O−H bond length from 0.99 to 1.11 Å. The product side adduct consists of the exothermic formation of a dative-bonded adduct similar to that found for the amine-terminated SAM. The overall reaction has a high exothermicity of 22 kcal/mol. Increasing the size of the precursor to TDMAT produced the same reaction mechanism with a hydroxyl-terminated SAM. The adsorption energy of the hydrogen-bonded complex was reduced to only 3.5 kcal/mol, but the activation energy and reaction energy were unchanged with respect to the hydrogen-bonded complex (Figure 3). This again suggests a reduced reactivity at low-pressure conditions with a change in the activation barrier with respect to the vacuum but invariance at high-pressure conditions. The low activation energy and large exothermicity suggest a much faster reaction on OH-terminated SAMs, compared to NH_2-terminated SAMs, borne out by the well-known high reactivity of Ti precursors to hydroxylation.

The reaction mechanism of the deposition of titanium tetramide on thiol-terminated SAMs is very similar to that on hydroxyl-terminated SAMs, with the formation of a weak hydrogen-bonded intermediate at the entry channel. The binding energy of the hydrogen-bonded complex is much lower, 2.5 kcal/mol, with a smaller S−H bond distortion compared to that of hydroxyl-terminated SAMs due to the lower electronegativity of the sulfur atom. The activation barrier relative to the weak hydrogen-bonded intermediate was found to be 9 kcal/mol, and the reaction was found to be exothermic with a reaction energy of 10 kcal/mol (Figure 2). In the transition state for thiols, the organometallic species retains a distorted tetrahedral structure in contrast to the trigonal-bipyramidal structures for amine- and

(45) Weiller, B. H. *J. Am. Chem. Soc.* **1996**, *118*, 4975−4983.

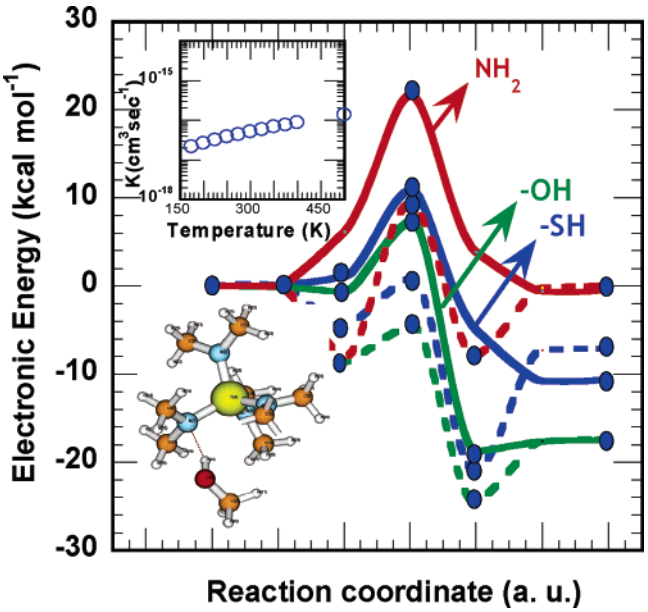

Figure 3. PED for deposition of TDMAT on $-NH_2$, $-OH$, and $-SH$ SAMs with key as in Figure 2. (Inset) Hydrogen-bonded structure of the physisorbed complex; temperature invariance for deposition on hydroxyl SAMs.

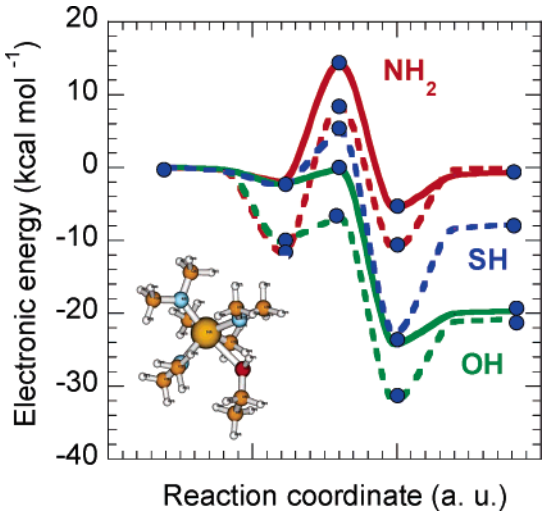

Figure 4. PED for the deposition of different metal precursors zirconium tetramide (dashed lines) and TDMAZ (solid lines) on amine SAMs using B3LYP/6-311++G(d,p)//B3LYP/6-311G(d). (Inset) Dative-bonded structure of the physisorbed complex for Zr on $-OH/SH$ SAMs.

hydroxyl-terminated SAMs, with elongation of the hydrogen-bonding ligand and nearly complete transfer of a proton from the thiol to the amine group in the hydrogen bond. This is accompanied by a large reduction in the Ti−S bond distance from 4.5 to 4.05 Å. This can be attributed to the much weaker S−H bond, with a dissociation energy of 80 kcal/mol compared to 94 kcal/mol for O−H and HN−H. Bond lengths for Ti−N and Ti−S of 1.90 and 2.33 Å, respectively, obtained in our calculations are in good agreement with experimental bond lengths obtained from X-ray structural data (1.92 and 2.39 Å, respectively).[46] For the bulkier precursor TDMAT, the adduct binding was observed to decrease by 2.5 kcal/mol, with a negligible change in the reaction exothermicity (Figure 3). The invariance of the activation barrier with respect to the vacuum and a decrease with respect to the adduct suggest a negligible effect of precursor size at low-pressure deposition and enhanced kinetics at high-pressure conditions for thiols. $TiCl_4$ was found to have a qualitatively similar reaction mechanism to that of titanium tetramide for amine SAMs.[44] Assuming similar behavior for $-OH$ and $-SH$ SAMs, the formation of a similar 1:1 molecular complex with no barrier has been observed experimentally for the reaction of $TiCl_4$ with CH_3OH and CH_3SH.[47] Further, it was observed that a complex with the hydroxyl group was unstable and rapidly reduced $TiCl_4$, consistent with our proposed mechanism of a barrier below the vacuum level. In contrast, they found the molecular complex formed with CH_3SH to be stable, in agreement with our proposed mechanism with its saddle point above the vacuum level. The lower activation energy and higher reaction energy of thiols compared to amines suggests that thiols will be better suited for lower-temperature deposition. Although thiols have slower kinetics compared to hydroxyl ligands, which have a barrierless deposition, an activation barrier above the vacuum level would allow for better control over the deposition process using parameters such as temperature.

We can find more information regarding the mechanisms by studying the variation in charge distribution within the molecule accompanying the structural distortions. A natural population analysis (NPA) method was used to analyze the charge distributions on individual atomic orbital components. Titanium tetramide has an effective charge of $-0.12\ e$ when it forms an adduct with an amine-terminated SAM, which is characteristic of a dative bond, compared to a slightly positive charge observed for the hydrogen-bonded adducts with hydroxyl- and thiol-terminated ligands, suggesting a distinct reaction intermediate involving charge loss from the metal center. The effective charge on the C_2H_5O and C_2H_5S groups in the entry-channel intermediates for $-OH$ and $-SH$ ligands increases from -0.45 to $-0.51\ e$ and from -0.11 to $-0.16\ e$, respectively, with a corresponding increase in the charge on transferring the hydrogen atom, indicating hydrogen bonding.

3.2. Effect of Changing the Metal Center to Zirconium. Replacing the metal center of the organometallic species from Ti to Zr does not alter the reaction mechanism for $-NH_2$ SAMs. The adduct binding energy increases by 6 kcal/mol, but the activation barrier with respect to this adduct is unchanged compared to that for a Ti precursor (Figure 4). Depositing the larger TDMAZ on $-NH_2$ SAMs causes the activation barriers with respect to the entry-channel adduct to decrease by 4 kcal/mol compared to that of zirconium tetramide (Figure 4). The reaction exothermicity is found to be similar to those for corresponding Ti precursors. These results suggest that, at low deposition pressures, Zr precursors should be kinetically more reactive than Ti precursors, but their equilibrium constant would remain unchanged. At high-pressure conditions, bulkier TDMAZ should have faster kinetics than TDMAT on amine SAMs. The reaction of Zr precursors on $-OH$ SAMs proceeds with the formation of a dative-bonded adduct for Zr, in contrast to the hydrogen-bonded intermediate for Ti (Figure 4, inset). Increasing the size from zirconium tetramide to TDMAZ causes the adduct binding energy to decrease by 5 kcal/mol (Figure 4). The

(46) Carmalt, C. J.; Dinnage, C. W.; Parkin, I. P.; White, A. P.; Williams, D. J. *J. Chem. Soc., Dalton Trans.* **2001**, *18*, 2554−2558.
(47) Ault, B. S. *J. Mol. Struct.* **1997**, *406*, 23−28.

activation barrier with respect to the adduct was found to decrease by 5 kcal/mol compared to that for Ti. These calculations predict a nearly barrierless deposition for Zr-based organometallic species on hydroxylated surfaces, which has been observed experimentally as facile ALD reactions of zirconium oxides from amido organometallic precursors.[49] The reaction of zirconium tetramide on thiol SAMs proceeds through the formation of weak dative-bonded intermediates, in contrast to the hydrogen-bonded intermediate for Ti with its distorted trigonal-bipyramidal structure. The activation barrier with respect to this adduct was found to be 6 kcal/mol, compared to 9 kcal/mol for Ti precursors (Figure 4). The overall reaction exothermicity was found to increase with increasing precursor size for Zr precursors. The increase in binding energy of the dative-bond adduct on amine SAMs and the change in the reaction mechanism of Zr for hydroxyl and thiol SAMs can be attributed to the higher electron affinity of zirconium.

3.3. Effect of Altering the SAM Backbone. The results above show the significant effect of the electronegativity of the terminal functional group in altering the reaction kinetics and mechanism of the deposition reactions of organometallic species. This suggests that alterations in the SAM backbone could be used to mediate the effect of the terminal group to produce a desired reactivity. In principle, fluoride-based ligands, with their high electronegativity, appear to be ideal charge-withdrawing groups for the SAM backbone that might induce a similar effect to amine-terminated groups and, thus, reduce the activation barrier. To investigate this idea for fluoride SAMs, we concentrated on substitution in amine-terminated groups, which have higher barriers. Depositing titanium tetramide on an amine-terminated group attached to a fluorocarbon SAM, whose backbone is represented by C_2F_5, we found that the reaction proceeds with the formation of a hydrogen-bonded intermediate similar to that found for hydroxyl SAMs and in contrast to the dative-bonded adduct for alkylamine SAMs. The adduct binding energy is 5 kcal/mol (Figure 5). The activation barrier with respect to this adduct was observed to reduce to 12 kcal/mol, compared to 18 kcal/mol for the corresponding deposition on alkyl SAMs (Figure 5).

This is accompanied by an increase in the exothermicity of the reaction by 5 kcal/mol with the formation of a more stable product due to a stronger Ti−fluoryl SAM ligand bond compared to that of alkyl SAMs, making the deposition kinetically and thermodynamically more favorable. Varying the chain length of the fluoryl backbone does not significantly alter the energetics, as we have already found for the alkyl SAMs. Replacing the β-CF_3 group on the backbone by an alkyl methyl group increases the adduct binding energy by 2 kcal/mol but does not change the barrier with respect to the vacuum, resulting in an increase in the barrier with respect to the adduct of 14 kcal/mol.

Reducing the extent of fluorine substitution in the backbone by depositing titanium tetramide on a fluoroalkene termination does not change the activation barrier and reaction exothermicity with respect to the adduct but increases the barrier by 3 kcal/mol with respect to the vacuum, suggesting that the deposition kinetics is more sensitive to fluorine substitution on the α-carbon

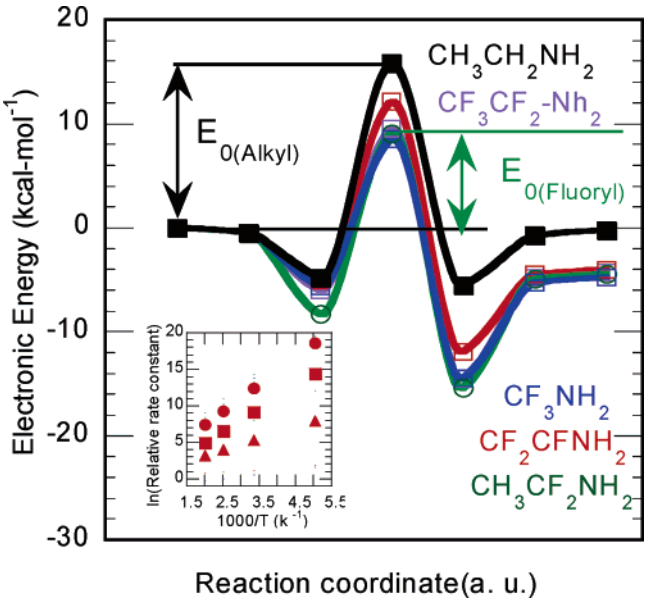

Figure 5. PED for deposition of titanium tetramide on various fluorinated SAMs in comparison to that corresponding to alkylamine (black line). (Inset) Rate constant for titanium tetramide on fluorylamine SAMs relative to alkylamine SAMs where △ = $-CF_2CF$, ○ = $-C_2F_5$, and □ = $-CH_3CF_2$ SAMs.

only. The increase in the activation barrier with a decrease in fluorine substitution toward a barrier similar to that of alkylamines suggests that deposition kinetics on the technologically important fluorylalkylamide (CF_3-$(CF_2)n$-CH_2-NH_2) SAMs would be similar to that on alkylamide SAMs but thermodynamically more favorable with a more stable product.

3.4. Surface Packing. SAM surfaces present multiple reactive groups to the incoming organometallic species. Neighboring groups can interact with the incoming organometallic to alter the reaction pathway and reaction energetics, such as the adsorption energies of adducts with long-range hydrogen bonding, from multiple sites. To evaluate these ideas, we have studied the deposition of titanium tetramide and TDMAT on model surfaces with a variety of SAM terminations. We have compared these to corresponding reactions in the gas phase to evaluate the differences caused by the surface. We have also investigated the possibility of unimolecular dissociation of TDMAT by forming imine or β-hydride elimination, forming metallacycles leading to Ti−C with a loss of dimethylamine ligand, as given by eqs 1 and 2, on all three SAM surfaces. The onset of these decomposition reactions for TDMAT in the gas phase has been reported at high temperatures (177−207 °C).[50−52]

$$XNH\cdot\cdot M(N(CH_3)_2)_2\cdot\cdot NHX \rightarrow XNH\cdot\cdot M(N(CH_3)_2)_2\cdot\cdot NX + NH(CH_3)_2 \quad (1)$$

$$XR\cdot\cdot M(N(CH_3)_2)_2\cdot\cdot RX \rightarrow XR\cdot\cdot(CH_2NCH_3)M\cdot\cdot\cdot RX + NH(CH_3)_2 \quad (2)$$

where R = O, S, NH.

(48) Fix, R.; Gordon, R. G.; Hoffman, D. M. *Chem. Mater.* **1991**, *3*, 1138−1148.
(49) Hausmann, D. M.; Kim, E. M.; Becker, J.; Gordon, R. G. *Chem. Mater.* **2002**, *14*, 4350−4358.
(50) Dubois, L. H.; Zegarski, B. R.; Girolami, G. S. *J. Electrochem. Soc.* **1992**, *139*, 3603−3609.
(51) Driessen, J. P. A. M.; Schoonman, J.; Jensen, K. F. *J. Electrochem. Soc.* **2001**, *148*, G178−G184.
(52) Amato-Wierda, C.; Norton, E. T., Jr. *Chem. Mater.* **2001**, *13*, 4655−4660.

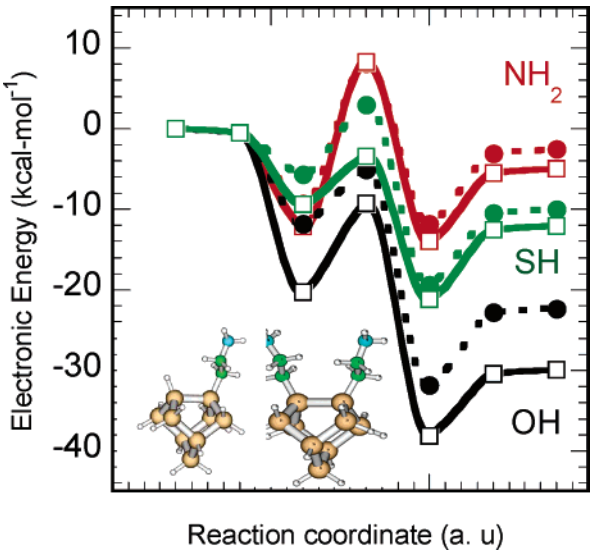

Figure 6. PED for the deposition of titanium tetramide on $-NH_2$, $-OH$, and $-SH$ SAMs (single SAM molecule per dimer = dashed lines and two SAM molecules per dimer = solid lines) attached to a Si_9H_{15} cluster modeling the surface, as shown in the insert.

Depositing titanium tetramide on amine and hydroxyl SAM molecules attached to a Si (100) surface with ~25% coverage gives reaction energetics and mechanisms similar to those of the corresponding gas-phase reaction. Next, we investigated the deposition of titanium tetramide on two SAM molecules on the Si (100) dimer and TDMAT on the diagonal dimer. When titanium tetramide was deposited on ethylamine attached to a Si (100) dimer, a dative-bonded adduct was formed with one of the SAM molecules, similar to that on a single SAM but with additional hydrogen bonding between the organometallic amine ligand and another SAM molecule. This led to an increased binding energy and an overall reaction energy of 4 kcal/mol (Figure 6). The activation barrier was found to be 8 kcal/mol with respect to the vacuum. This would lead to slower deposition kinetics in high-pressure deposition conditions. Once deposited, the activation barrier for the reaction with a second terminal group was found to be 14 kcal/mol relative to the vacuum, with the overall reaction being endothermic. When titanium tetramide was deposited on ethanol and ethylthiol SAMs attached to the Si dimer, the adduct formation energy was found to nearly double with the formation of multiple hydrogen bonds (Figure 6), increasing the probability of precursor-mediated deposition. The activation barrier with respect to this intermediate for hydroxyl-terminated SAMs was found to increase from 7 to 11 kcal/mol for single site deposition. The overall reaction exothermicity increases from 22 to 30 kcal/mol. This suggests an increase in thermodynamic favorability but a reduction in kinetic favorability. The activation barrier for thiol-terminated SAMs with respect to the adduct was found to be unchanged, but the overall reaction energy was found to increase by 2 kcal/mol, increasing the thermodynamic favorability.

We investigated the deposition of TDMAT on a "diagonal dimer" surface for adsorption and unimolecular side decomposition reactions, as shown by the schematic in Figure 7. The reaction mechanism and PED for the deposition of TDMAT on amine SAMs on a diagonal dimer is similar to that for the corresponding gas-phase reaction. The activation barrier of 19 kcal/mol relative to the physisorbed complex agrees with experimental data for the surface-limited reaction of TDMAT.[25] As noted earlier, DFT methods capture trends in physisorbed complexes and changes in activation barriers relative to these complexes fairly accurately but underestimate the absolute values. Correcting for this underestimation with MP2/6-311G-(d), we found the activation barrier for TDMAT on amine SAMs relative to the vacuum to be 9.5 kcal/mol (Figure 8). The activation barrier and reaction endothermicity for the second site reaction was found to increase by 4 and 9 kcal/mol using B3LYP/6-311G(d) and MP2/6-311G(d), respectively. Taking into account the entropic changes in free energy calculations, we found the second site reactions to have comparable free-energy changes to the first site reactions for amine SAMs at temperatures as low as 200 K (Figure 8 and further illustrated in Figure 10). Thus, at low temperatures also, each TDMAT molecule reacts with multiple sites with the loss of two dimethylamine molecules.[53,54] The desorption energy for the byproduct dimethylamine, produced after the second site deposition, was found to be 29 kcal/mol using MP2/6-311G(d), which is in very good agreement with the experimental value of 29.1 kcal/mol at low coverage.[55] This would result in the buildup of dimethylamine on a growing TiN surface and contribute to nonconformal growth,[54] necessitating an increase in the purge cycle time and gas flow rate.

We also evaluated the kinetics of the unimolecular reactions expressed by eqs 1 and 2. Compared to the second site reaction barrier of 23 kcal/mol, the activation barrier for an imine formation reaction, after initial TDMAT deposition on the surface, was found to be 38 kcal/mol (Figure 9). The free energy change for imine formation from the deposited TDMAT relative to the free-energy penalty for TDMAT deposition in the gas phase suggests that imine formation reactions are unfavorable below 400 K, at least for the packing of the SAM chosen here. Sparsely packed SAMs could make imine formation more competitive than a multiple site reaction due to the increased entropic penalty in the latter. After the second site reaction, the deposited TDMAT molecules can again dissociate as governed by eq 1 or 2. Imine formation, with an activation barrier of 30 kcal/mol, was found to be kinetically and thermodynamically more favorable than metallacycle formation, with an activation barrier of 40 kcal/mol (Figure 9), and kinetically comparable to the second site deposition around 300 K. This would reduce the Ti−N ratio from 1:4 to 1:3 around 300 K. The activation barrier necessary for further imine reaction to form two imine bonds (hence reducing the Ti−N ratio to 1:2) was found to be 45 kcal/mol. However, the desorption energy of the byproduct dimethylamine was found to nearly double compared to that of the first imine formation, making the reaction thermodynamically limited as compared to the latter reaction.

According to the TST, the kinetics of a reaction is proportional to the free energy of the activated complex relative to the stable reactants.[56] This allows us to incorporate entropic as well as enthalpic effects in the form of a free-energy barrier of the activated complex, making it easier to compare bimo-

(53) Killampalli, A. S.; Ma, P. F.; Engstrom, J. R. *J. Am. Chem. Soc.* **2005**, *127*, 6300−6310.
(54) Elam, J. W.; Schisky, M.; Ferguson, J. D.; George, S. M. *Thin Solid Films* **2003**, *436*, 145−156.
(55) Okada, L. A.; George, S. M. *Appl. Surf. Sci.* **1999**, *137*, 113−124
(56) Steinfeld, J. I.; Francisco, J. S.; Hase, W. L. *Chemical Kinetics and Dynamics*, 2nd ed.; Prentice Hall: New Jersey, 1998; p 301.

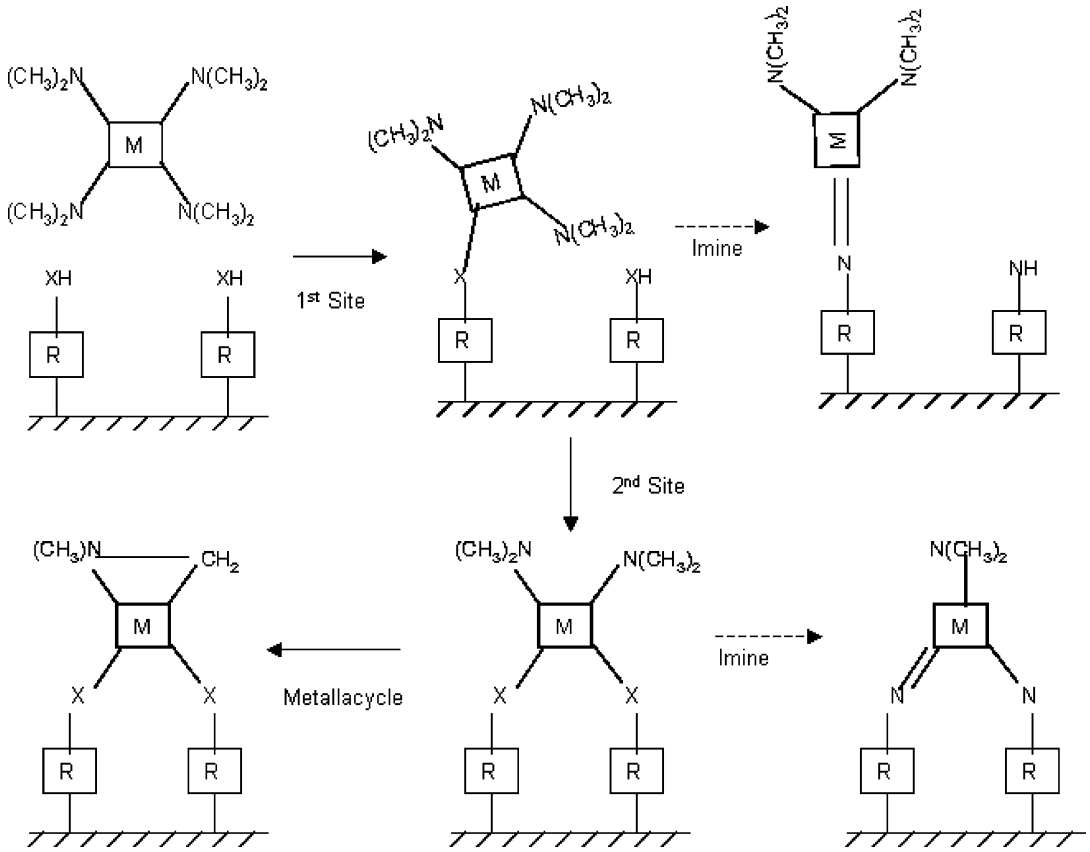

Figure 7. Schematic diagram of the surface reactions of TDMAT on SAM surfaces. X refers to the terminal functional group (−O; −S; −NH); M = Ti and R = alkyl chain.

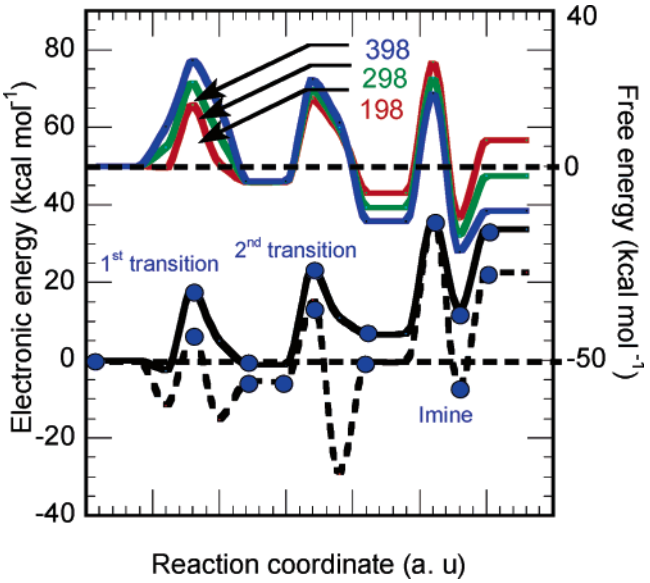

Figure 8. PED for the deposition of TDMAT on $-NH_2$ SAMs attached to an Si diagonal dimer using B3LYP/6-311+G(d,p)//B3LYP/6-311G(d) (solid black line) and MP2/6-311G(d)//B3LYP/6-311G(d) (dashed black lines). Free-energy plots for the corresponding reactions over 198−398K at 0.001 atm are shown above (red = 198 K, green = 298 K, and blue = 398 K).

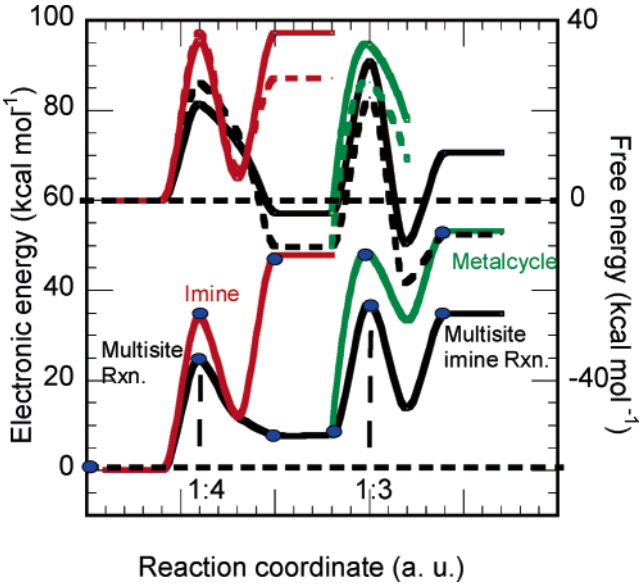

Figure 9. PED and free-energy diagram for the unimolecular side reactions of deposited TDMAT on amine SAMs attached to an Si diagonal dimer at B3LYP/6-311G(d). Free-energy plots on top correspond to 198 K (solid line) and 398 K (dashed line) for the corresponding reactions.

lecular and unimolecular reactions on the same basis. Thus, to accurately study the kinetic favorability of various steps of TDMAT deposition and decomposition as a function of temperature, we have investigated the variation in free energy of activation ($\Delta G^{\ddagger}$) with temperature (T), $\Delta G^{\ddagger}/T$, normalized to the corresponding value for the gas phase β-hydride elimination reaction known to occur at 480 K.[50−52] Thus, any reaction with a normalized value of $\Delta G^{\ddagger}/T$ less than 1 is assumed to be kinetically favorable at that temperature.

We found the activation barrier for gas phase β-hydride elimination given by eq 2 to be 39.5 kcal/mol, which is in good agreement with the experimental value of 39.7 kcal/mol.[52] The same dissociation reaction on an amine substrate is predicted,

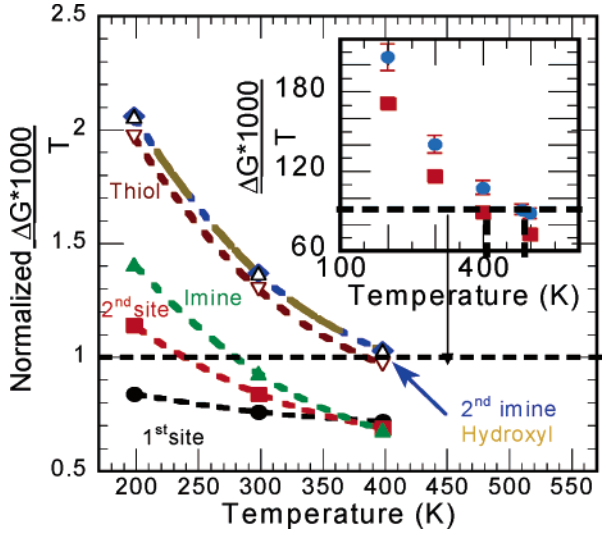

Figure 10. $\Delta G^{\ddagger}/T$ vs temperature. (Insert Results for gas-phase decomposition via β-hydride elimination (blue diamonds) compared with that on an amine surface (red squares).

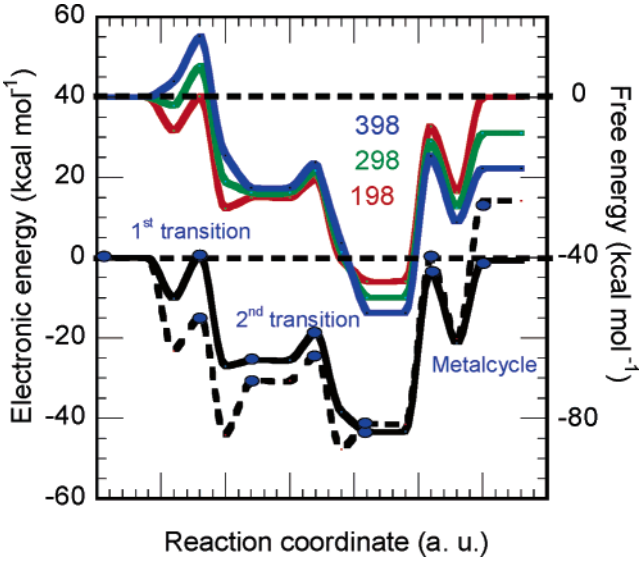

Figure 11. PED and free-energy diagram for the deposition of TDMAT on −OH SAMs attached to a Si diagonal dimer. Free-energy plots above correspond to 198−398 K at 0.001 atm. Key as in Figure 8.

by our calculations, to occur with a lower activation barrier of 33 kcal/mol and, hence, is favorable at the lower temperature of ∼400 K (Figure 10, inset). Accordingly, we studied the temperature range 198−398 K. Figure 10 shows that multisite reactions of TDMAT on amine SAMs are favorable at temperatures above 220 K. Subsequent imine formation reactions are kinetically only favorable above 300 K. Multiple imine formation is favorable only around 400 K, where TDMAT decomposition also starts. As we increase the temperature from 220 to 400 K, we would expect the Ti−N ratio to decrease from 1:4 to 1:3 to 1:2. This agrees with recent experiments by Killampalli et al.[53] As observed from Figure 9, metallacycle formation becomes competitive with imine formation beyond 400 K, resulting in increased carbon incorporation in the growing film as "carbidic" Ti−C with the loss of three ligands. This suggests that processing temperatures should be kept below 400 K for low carbon films, in agreement with QCM studies and FTIR experiments by Elam et al.,[54] who found an increase in carbon contamination with increasing temperature with the hypothesis of a loss of 2.5−3 dimethylamine groups for temperatures above 120 °C (∼400 K).

On hydroxyl SAMs, the adduct binding energy nearly doubled from the corresponding gas phase values to 12 kcal/mol with multiple hydrogen bonding. The activation barrier increased to 11 kcal/mol relative to the intermediate, and the reaction exothermicity increased to 30 kcal/mol, similar to that for the dimerized Si surface (Figure 11). The transition state was found to be 13.6 kcal/mol below the vacuum level, which is in good agreement with the recent experimental value of 13.0 ± 4.0 kcal/mol below the vacuum level for the deposition of TDMAT on chemical oxide.[53] This validates our precursor-mediated chemisorbed mechanism with a transition state below the vacuum level for hydroxyl SAMs, verified by the free energy plots. The activation barrier for the second site reaction decreased by 4 kcal/mol compared to that of the reaction with the first site, in contrast to a corresponding increase for the amines. Subsequent decomposition via β-hydride elimination is found to be kinetically limited below 400 K. The activation barrier for β-hydride deactivation after multiple site reactions was found to be 42 kcal/mol, with respect to multiple site reaction products, or 12 kcal/mol, with respect to the entry-channel adduct. Thus, we would not expect the Ti−N ratio to be 1:1 below 400 K (Figure 10). In addition, the binding energy of the byproduct dimethylamine was found to be 12 kcal/mol, which is ∼15 kcal/mol less than amine SAMs, reducing purge-cycle time. It is also noticeable that there is a much higher kinetic and thermodynamic propensity for multiple site reactions on hydroxyl SAMs compared to that on amine SAMs for either surface packing density. This suggests that, even at very low temperatures, TDMAT molecules could lose multiple ligands on hydroxyl SAMs (Ti−O ratio of 1:2) without self-dissociation. This has been confirmed by recent experimental results.[53] On thiol SAMs, the reaction mechanism and PED for the first site reaction are very similar to those of the corresponding gas-phase reaction. The activation barrier with respect to the entry-channel adduct was found to be lowered to 5 kcal/mol (8 kcal/mol for gas phase) with a reaction exothermicity of 9 kcal/mol (Figure 12). Thus, at high pressures, thiol SAMs would be kinetically most favored for TDMAT deposition. The activation barrier for the second site reaction was found to increase significantly to 18 kcal/mol, but it is still equivalent to the barrier found for amines. The overall reaction is exothermic with a reaction energy of 10 kcal/mol. From the free-energy plots in Figure 12, we again find multiple site reactions to be favorable above 200 K. Thus, even at low temperatures, multiple site reactions are kinetically and thermodynamically more favored on thiol SAMs than on amine SAMs. This reduces the amount of TDMAT precursor pressure required to push the forward reaction and would decrease subsequent purge time due to the reduced binding energy of the dimethylamine group.

The potential energy surface for hydroxyl SAMs, obtained above, suggests a significant effect of surface distribution of sites. The currently chosen ethylamine SAM cluster may not provide enough degrees of freedom to the TDMAT precursor to allow other possible configurations for different underlying substrates or more flexible longer chains. To overcome this, we studied the corresponding gas phase reaction between TDMAT and two ammonia molecules. Elam et al.[54] found that, at low temperature, TiN ALD and CVD share a common rate-

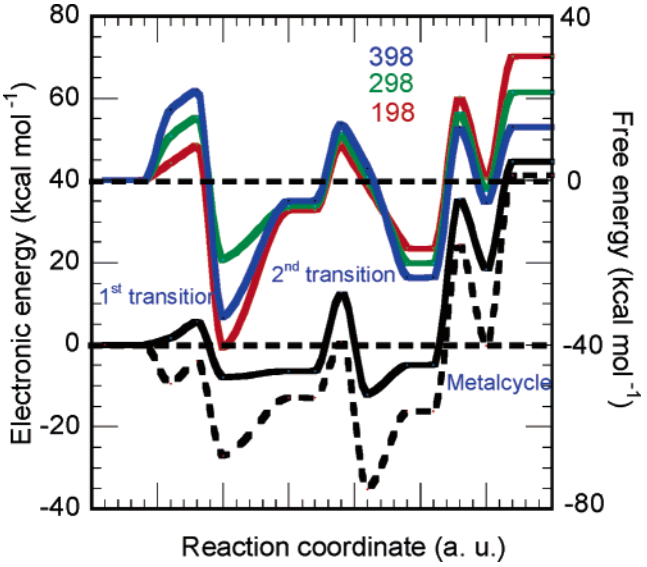

Figure 12. PED and free-energy diagram for the deposition of TDMAT on −SH SAMs attached to a Si diagonal dimer. Free-energy plots on top correspond to 198−398 K at 0.001 atm. Key as in Figure 8.

limiting step. In the presence of two ammonia molecules, the reaction was observed to proceed through the formation of a doubly dative-bonded complex with a similar binding energy. However, the activation barrier with respect to this adduct was observed to be reduced to 13 kcal/mol, analogous to that of hydroxyl SAMs, suggesting catalysis by the second amine (Figure S1; Supporting Information). This would result in an activation barrier of 1−2 kcal/mol relative to the vacuum, which is in good agreement with the experimental value of 2−4 kcal/mol at low pressures on surfaces.[54]

3.5. Trends in Reactivity and Kinetics. We calculated the reaction rate constant for these gas phase reactions using the conventional TST with Wigner's tunneling coefficient. The reaction rate expression from TST is given by[59]

$$k = \tau\left(\frac{k_n T Q_t^{\ddagger}(T)}{hQ_r(T)}\right)\exp\left(-\frac{E_a}{RT}\right) \quad \text{where} \quad \tau = 1 + \frac{1}{24}\left(\frac{h\upsilon}{k_b T}\right) \quad (3)$$

and τ is Wigner's tunneling coefficient, $Q^{\ddagger}$ and Q are the overall partition functions of the transition state and the reactants, respectively, and E_a is the activation energy relative to the reactants. The rate constants were calculated between 200 and 500 K, the thermal stability range for SAMs. The experimentally observed insensitivity to temperature dependence for the deposition of TDMAT on −OH SAMs was also observed in our calculations (Figure 3, inset).[53] We can also see that α-carbon fluorinated SAMs are kinetically and thermodynamically most favored for low temperature deposition (Figure 7, inset).

In our surface rate calculations, the physisorbed adduct complexes were considered as the reactants with two degrees of translational freedom for thiol and hydroxyl SAMs (a precursor-mediated diffusion) on the basis of their PED for surface reactions and negligible structural distortions of physisorbed adducts. The adduct on amine-SAMs was assumed to lose all translational freedom, owing to a distorted geometry datively bonded. The activated complex on the surface is assumed to have contributions only from the vibrational partition function for all SAM surfaces, because the organometallic precursors are immobilized on the surface, leaving no translational moves. We assume a fast, barrierless physisorption step in equilibrium with a gaseous precursor, such that the adduct-to-activated complex is the rate limiting step. For such deposition conditions, occurring at high precursor partial pressure, the rate constant for precursor-mediated deposition could be approximated by (discussed in Supporting Information):

$$k_r = \tau\left(\frac{k_n T(Q_t^{\ddagger}(T))_v}{h(Q_{TDMAT-trans}(T))^{0.66} * Q_{rot} * (Q_{TDMAT-surface}(T))_v}\right) \times \exp\left(-\frac{E_a}{RT}\right) \quad (4)$$

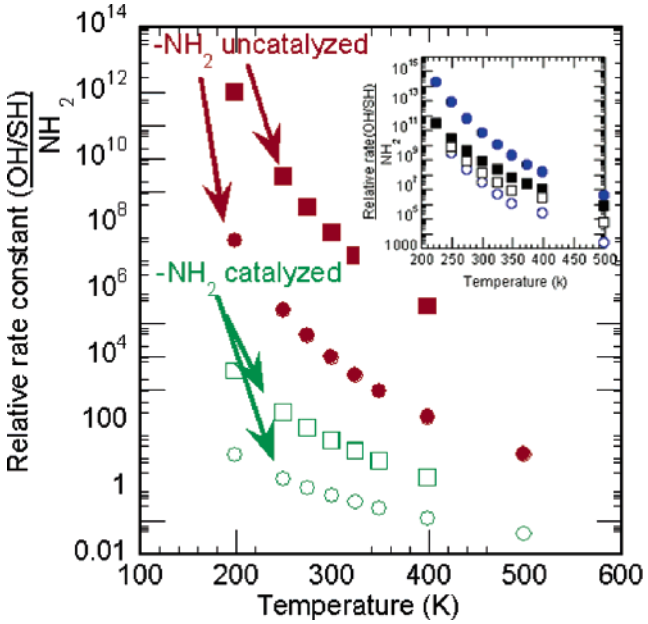

Figure 13. Relative rate constants with respect to the physisorbed adduct (Circles: −OH SAMs; squares: −SH SAMs). Green and red: Surface-mediated rate constants. (Inset) Corresponding gas-phase relative rates with respect to the vacuum (low pressure) (filled symbols) and adduct (high pressure) (open symbols)

The variation in the rate constants of TDMAT deposition on −OH and −SH SAM surfaces with respect to the physisorbed adduct has been plotted relative to the rate constant on −NH_2 SAMs (Figure 13). From Figure 13, thiol SAMs surfaces are found to be kinetically much more favorable than hydroxyl surfaces over the whole temperature range. This contrasts sharply with the result for the corresponding gas phase reaction, where a negligible difference was observed between the relative rates for hydroxyl and thiol terminal groups. This clearly illustrates the ability of a surface to alter the deposition kinetics significantly. We have also plotted the rate constant relative to catalyzed TDMAT deposition on an amine surface. For surface-catalyzed reactions, amine SAMs are found to be kinetically comparable to hydroxyl SAMs, in agreement with recent experiments by Killampalli et al.[53] We also calculated the kinetics at low coverage and low precursor partial-pressure

(57) Ruhl, G. R.; Rehmet, R.; Knizŏvá, M.; Merica, R.; Vepřěk S. *Chem. Mater.* **1996**, *8*, 2712−2720.
(58) Baev, A. K.; Mikhailov, V. E. *Russ. J. Phys. Chem.* **1989**, *63* (7), 949−955.
(59) Reid, D. L.; Shustov, G. V.; Armstrong, D. A.; Rauk, A.; Schuchmann, M. N.; Akhlaq, M. S.; Sonntag, C. V. *Phys. Chem. Chem. Phys.* **2002**, *4*, 2965−2974.

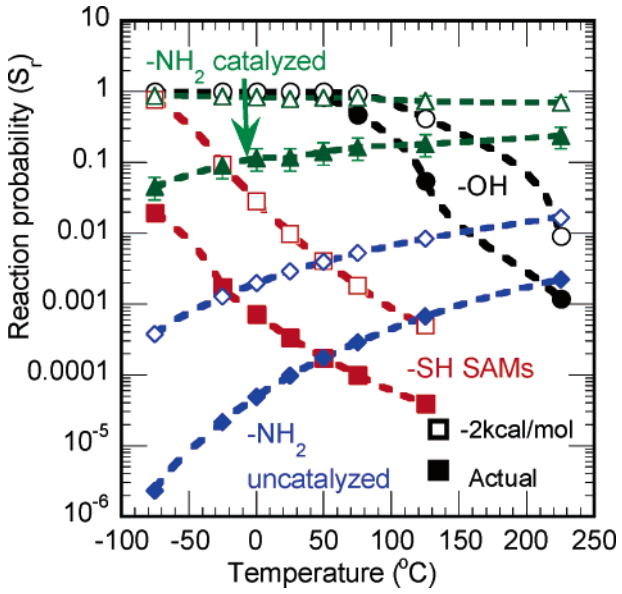

Figure 14. Initial reaction probability of TDMAT on various SAM surfaces. Closed symbols: actual value from the calculations; Open symbols: incorporation of a −2 kcal/mol uncertainty in the activation barrier.

deposition conditions, such as ultrahigh vacuum deposition, where the desorption of the physisorbed complex could become competitive with dissociative chemisorption. Assuming a pseudosteady state at the adduct, the initial reaction probability (S_r) is given by[60]

$$S_r = \tau\left(\frac{k_r}{k_r + k_d}\right) \quad \text{where} \quad k_d = 10^{13}\exp\left(-\frac{E_a}{RT}\right) \qquad (5)$$

and τ is the trapping probability (assumed to be equal to 1); the desorption prefactor is assumed to be 10^{13}. We have also looked at the effect on the rates of an uncertainty of ±2 kcal/mol (that inherent in the calculations) in the activation barrier calculations (Figure 14). This sensitivity analysis provides us with reasonable upper and lower bounds for expected relative rates between the two SAMs for the assumed reaction mechanisms. At low deposition pressures, the initial reaction probability for hydroxyl and thiol SAMs is found to decrease with an increase in temperature, characteristic of precursor-mediated deposition with an activated state below the vacuum level, as compared to an increasing probability for uncatalyzed deposition on amines SAMs. This is in agreement with recent experiments for TDMAT deposition on chemical oxide surfaces.[61] Hydroxyl SAMs are found to be kinetically most favorable up to ~425 K, with near unit reaction probability, at which point they become comparable to amine SAMs.

At low surface coverage, for deposition on a well-packed amine SAM surface, we would expect catalysis from the surface, which would result in a nearly constant reaction probability of 0.1−0.2 at the lower bound. This is in very good agreement with the experimental value of 0.25[53] and should be compared to a value 3−4 orders of magnitude lower for uncatalyzed deposition. These results suggest that the experimental deposition mechanism is catalyzed and again reflects the very significant influence of surface functional groups and packing density to alter deposition kinetics. Thiol SAMs are kinetically more favorable than amine SAMs for uncatalyzed reactions below 325 K, which is only possible if the amine SAMs are sparsely packed. This makes thiol SAM surfaces unsuitable for low-pressure deposition, as compared to being the most favorable substrate for high-pressure deposition. This demonstrates the influence of deposition conditions on the choice of substrate.

4. Conclusions

We have systematically studied reaction kinetics for the initial layer deposition of Ti- and Zr-based alkylamide organometallic precursors on alkyltrichlorosilane SAMs with different terminal groups using DFT methods. For both metal centers, we found the initial reaction rate constant for deposition to decrease in the order OH > SH > NH_2, which is consistent with experiments.[53] Reactions on hydroxyl SAMs were found to proceed with the saddle point below the vacuum level. Thiol SAMs were observed to have lower ligand-exchange barriers, despite less stable intermediates, due to the weaker bond strength of the thiol bond. These results suggest a precursor-mediated deposition for both surfaces, verified by kinetics calculations at low deposition pressures. On the basis of kinetic and thermodynamic favorability, Zr-based precursors were found to be more suitable for faster deposition. The deposition kinetics were observed to be independent of the length of the SAM molecule but influenced by the size of the organometallic precursor. There is a reduction in stability of the complex intermediates with increasing precursor bulkiness. The surface packing of SAM molecules was found to have a significant effect on the stability of the complex intermediates, activation barriers, and localized bonding of the organometallic, especially for hydroxyl-terminated SAMs. At low temperatures, we expect TDMAT to lose multiple side ligands ($-N(CH_3)_2$) on all SAM surfaces, leading to multiple bonding sites. We have also studied the kinetics of competing side reactions, which define the developing surface. On amine SAMs, decomposition via multiple imine bond formation was found to be kinetically and thermodynamically favorable when the temperature was increased. Metallacycle formation via β-hydride elimination was found to be thermodynamically limited below 400 K, suggesting that this is an upper processing temperature limit to prevent incorporation of "carbidic" Ti−C. This reaction was thermodynamically most limited on thiol SAMs, which were also found to be kinetically favorable under high-pressure deposition conditions but unfavorable for low-pressure deposition. At low deposition conditions, hydroxyls were found to be most favored with a nearly constant reaction probability up to 375 K. At low coverage, deposition on an amine SAM surface was found to proceed through a surface-catalyzed pathway with a nearly constant reaction probability and comparable to a hydroxyl surface beyond 425 K, demonstrating the importance of the packing density of the SAM and the surface in altering the deposition kinetics. Amine SAMs with fluorine in the backbone were found to be kinetically and thermodynamically much more favorable than corresponding straight-chain SAMs. This demonstrates that it is possible to "engineer" the SAM backbone to increase the deposition kinetics on a desired terminal group.

Acknowledgment. We acknowledge financial assistance from the National Science Foundation for a NIRT award for Inorganic-Organic Interfaces (NSF-ECS-0210693) and the

(60) Lam, A. M.; Zheng, Y.-J.; Engstrom, J. R. *Surf. Sci.* **1997**, *393*, 205−221.
(61) Ma, P. F.; Engstrom, J. R. Personal communication.

Semiconductor Research Corporation via the Center for Advanced Interconnect Science.

Supporting Information Available: Tables of the input energies (kcal/mol) plotted in the figures are given with the relevant chemical structure; Cartesian coordinates of the final optimized structures for the surface studies depicted in Figures 8−13 with their electronic energies given in hartrees. This information is available free of charge via the Internet at http://pubs.acs.org.

JA054685K